

# Parametric Oscillation of a Moving Mirror Driven by Radiation Pressure in a Superconducting Fabry-Perot Resonator System

Raymond Y. Chiao<sup>a</sup>, Luis A. Martinez<sup>b</sup>, Stephen J. Minter<sup>c</sup>, and Alexey Trubarov<sup>c</sup>

<sup>a</sup>University of California, Merced, Schools of Natural Sciences and Engineering, P.O. Box 2039, Merced, CA 95344, USA

Corresponding author, email: rchiao@ucmerced.edu

<sup>b</sup>University of California, Merced, School of Natural Sciences, P.O. Box 2039, Merced, CA 95344, USA

<sup>c</sup>Vienna Center for Quantum Science and Technology, Faculty of Physics,  
University of Vienna, Boltzmannngasse 5, A-1090 Vienna, Austria

PACS: 42.50.Pq, 42.79.Gn, 07.57.Hm, 03.70.+k, 11.10.-z, 03.65.-w, 42.50.Xa

**Abstract:** A moving pellicle superconducting mirror, which is driven by radiation pressure on its one side, and by the Coulomb force on its other side, can become a parametric oscillator that can generate microwaves when placed within a high-Q superconducting Fabry-Perot resonator system. A paraxial-wave analysis shows that the fundamental resonator eigenmode needed for parametric oscillation is the  $TM_{011}$  mode. A double Fabry-Perot structure is introduced to resonate the pump and the idler modes, but to reject the parasitic anti-Stokes mode. The threshold for oscillation is estimated based on the radiation-pressure coupling of the pump to the signal and idler modes, and indicates that the experiment is feasible to perform.

## I. INTRODUCTION

Parametric oscillators for generating electromagnetic microwaves might be possible, based upon the idea that a moving mirror is like a moving piston that can perform work *nonadiabatically* on radiation contained within a cavity. Above a certain threshold, the parametric action of the moving mirror will exponentially amplify this radiation until it can become a large-amplitude, classical wave. An essential component for such a parametric oscillator is a high-Q superconducting (SC) resonator, which can be formed by a fixed, spherical curved SC mirror in conjunction with a moving, flat SC mirror (see Figure 1).

To understand how the proposed parametric oscillator works, let us imagine performing a thought experiment in which some weak, on-resonance, “seed” microwave radiation from an outside microwave source, is injected backwards through the output hole of the curved SC mirror of Figure 1, into the volume of the cavity between the curved and flat mirrors. Thus the SC resonator can

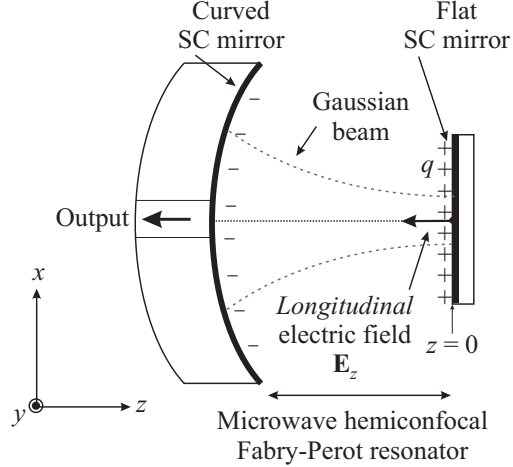


FIG. 1: Hemiconfocal Fabry-Perot superconducting (SC) resonator with electrostatically charged mirrors, for generating microwaves in a parametric oscillator. A Gaussian beam mode focused by a curved mirror onto a flat mirror with charge  $q$  that can move back and forth parallel to the  $z$  axis, yields a longitudinal electric field  $\mathbf{E}_z$  satisfying conducting boundary conditions. The lowest mode of the resonator is the transverse magnetic  $\text{TM}_{011}$  mode (see Appendix A).

be filled with “seed” radiation, exciting it into its fundamental  $\text{TM}_{011}$  eigenmode. As a result, there will appear a longitudinal electric field  $\mathbf{E}_z$  at the surface of the SC flat mirror that will be oscillating at the  $\text{TM}_{011}$  eigenmode frequency, i.e., at a microwave frequency (see Appendix A).

Next, imagine that the flat SC mirror consists of a thin SC film sputtered onto the left side of a thin, light, flexible diaphragm (e.g., the pellicle mirror to be introduced later in Figure 4), which is sufficiently thin so that this diaphragm can easily be driven into mechanical motion. Moreover, imagine that this film is electrostatically charged with a DC charge  $q$ . Then the longitudinal electric field  $\mathbf{E}_z$  at the surface of the SC film will lead to a force

$$\mathbf{F}_z(t) = q\mathbf{E}_z(t) \quad (1)$$

oscillating at the *same* microwave frequency as that of  $\mathbf{E}_z(t)$ . Note that (1) is a *linear* relationship between the force  $\mathbf{F}_z(t)$  and the electric field  $\mathbf{E}_z(t)$ . In this way, a force oscillating at a microwave frequency can be exerted upon the diaphragm parallel to the  $z$  axis, and the flat SC mirror will be driven into simple harmonic motion at the same microwave frequency as that of the  $\text{TM}_{011}$  eigenmode of the SC resonator of Figure 1.

Now consider the opto-mechanical configuration sketched in Figure 2, in which a laser beam from the right is incident on a moving mirror (e.g., on the flat SC mirror of Figure 1 with mul-

tilayer dielectric optical coatings deposited on its right side). When this moving optical mirror is combined with a fixed optical mirror in an optical Fabry-Perot-cavity configuration, there will arise a production of Doppler sidebands, which can then be utilized either for the laser cooling of the moving mirror by means of a *red-detuned* laser tuned to the lower Doppler sideband [1], or for the parametric oscillation of the moving mirror excited in an elastic mode at acoustical frequencies by means of a *blue-detuned* laser tuned to the upper Doppler sideband [2]. Above the threshold for parametric oscillation of the moving mirror within the SC resonator of Figure 1, a “signal” wave would begin to build up, growing exponentially with time starting from the injected “seed” microwave radiation. However, once parametric oscillation above threshold has occurred, one could turn off the source of the “seed” radiation. The SC resonator would then continue to oscillate as an autonomous source of the same microwaves as the “seed” in the absence of the “seed”, just like the autonomous generation of microwave radiation by the original ammonia maser above its oscillation threshold [3].

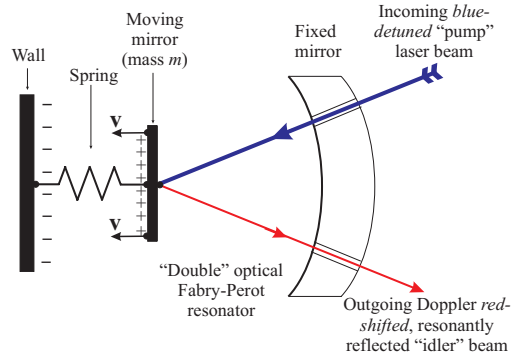


FIG. 2: A mass-and-spring model for an opto-mechanical parametric oscillator that could generate microwave radiation starting from “seed” radiation. The SC Fabry-Perot microwave resonator in Figure 1 is modeled by a charged mass attached via a spring to a fixed, charged wall. The “pump” laser beam (in blue) is *blue-detuned* so as to coincide with the *upper* Doppler sideband arising from the simple harmonic motion of the moving mirror. After reflection from the moving mirror, the laser beam is red-shifted to become the “idler” beam (in red), whose frequency coincides with the *lower* Doppler sideband. The “pump” laser beam will exert a radiation pressure force that will drive the mirror into parametric oscillations. Here the “Double” optical Fabry-Perot resonator represents a simplified model for the doubly-resonant structure depicted in Figure 3, which serves to resonate both the “idler” and the “pump” frequencies, but to reject the any Doppler up-shifted frequencies.

## II. OPTO-MECHANICAL MODEL FOR PARAMETRIC OSCILLATORS

For ease of understanding, consider the simplified opto-mechanical model for the parametric process shown in Figure 2, in which a moving mirror attached to a spring is coupled via radiation pressure to a strong “pump” laser at frequency  $\omega_p$ , a weak “idler” light wave within an optical resonator at frequency  $\omega_i$ , and a weak “signal” wave in the SC resonator at frequency  $\omega_s$ , which is being represented as a simple harmonic oscillator with a resonance frequency  $\omega_s$ , such that

$$\omega_p = \omega_i + \omega_s \quad (2)$$

The energy for the oscillating fields at  $\omega_i$  and  $\omega_s$  comes from the energy supplied by the pump laser at  $\omega_p$ .

In Figure 2, we have replaced the hemiconfocal microwave resonator shown in Figure 1 by a mass-and-spring model, in which the simple harmonic mechanical motion of the flat SC mirror of Figure 1 driven in the presence of the charge  $q$  by the longitudinal electric field  $\mathbf{E}_z(t)$  parallel to the  $z$  axis, is modeled by the simple harmonic motion of a mass attached via a spring to the fixed wall on the left side of Figure 2. The justification for using this mechanical model (see Appendix B) is that we have found that the fundamental eigenmode solution of the SC hemiconfocal microwave resonator, which is the Gaussian-beam  $\text{TM}_{011}$  mode, possesses a longitudinal component  $\mathbf{E}_z$  of the electric field which has a nonvanishing component along the  $z$  axis of the resonator acting on the electrostatic charge  $q$  at the surface of the flat mirror of Figure 1. Therefore there exists a longitudinal component of the force that drives the flat mirror back and forth into simple harmonic motion along the  $z$  axis, whose motion can then be simulated by the mass-and-spring model of Figure 2.

Furthermore, we shall model, by means of a single, simplified Fabry-Perot structure on the right side of Figure 2, a “Double” optical Fabry-Perot resonator, which is depicted in more detail in Figure 3, whose purpose is to simultaneously resonate both the strong, incoming *blue-detuned* laser (i.e., the “pump” laser) and the weak, Doppler red-shifted “idler” light wave produced upon reflection from the moving mirror, but whose purpose is also to serve as a rejection filter to reject any undesirable Doppler blue-shifted (or “anti-Stokes”) light. Later, we shall put all these pieces of the parametric oscillator system together in Figure 4.

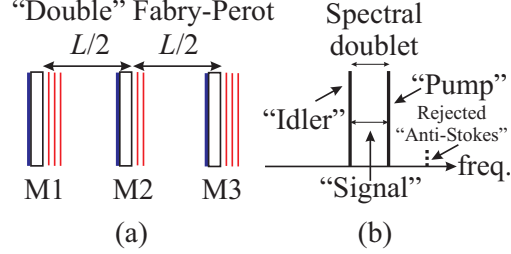


FIG. 3: (a) “Double” Fabry-Perot is a three-mirror resonator system with three equally spaced mirrors M1, M2, and M3. The leftmost mirror M1 is the flat, moving mirror attached to the spring of Figure 2, i.e., the “pellicle-mirror” of Figure 4. The pump laser is incident from the right through the rightmost mirror M3. Multi-layer dielectric coatings are indicated by red lines; anti-reflection coatings by blue lines. The reflectivity of M2 is less than that of M1 and M3. (b) The spectral transmission of this resonator system has a doublet structure, whose splitting is proportional to the transmittivity of the middle mirror M2. The frequency of the “pump” laser of the parametric oscillator coincides with the upper member of the doublet, and the frequency of the “idler” (“Stokes”) wave coincides with the lower member. The doublet splitting frequency is resonant with the “signal” frequency of the parametric oscillator. The parasitic “Anti-Stokes” wave is rejected by the structure.

### III. THE “DOUBLE” FABRY-PEROT RESONATOR

Figure 3(a) shows the detailed structure of the “Double” Fabry-Perot resonator, which consists of three equally spaced mirrors M1, M2, and M3. Suppose that M1 is the moving mirror of Figure 2 (or the “pellicle mirror” of Figure 4). Suppose further that at  $t = 0$  light initially fills the left half of the structure between M1 and M2, but that there is initially no light in the right half between M2 and M3. Then after a period of time determined by the transmittivity of the middle mirror M2, light will leak from the left cavity to the right cavity, until light fills the right cavity. This results in a periodic sloshing back and forth of the light between the left and right halves of the structure at a frequency equal to the splitting frequency of the spectral doublet shown in Figure 3(b). The “pump” laser will be tuned into the resonance with the upper member of the spectral doublet; the “idler” wave to the lower member of this doublet. Any small amount of noise at the idler frequency will lead to a radiation pressure force on the moving mirror M1 that will be modulated at the doublet splitting frequency, which can be chosen to be tuned into resonance with the SC microwave resonator frequency of Figure 1. This then can lead to a mutual, resonant reinforcement of the noise in the “idler” and “signal” modes that leads to exponential growth of both by parametric

amplification, and possibly to oscillation above a certain threshold, as will be presently shown.

An important feature of the “Double” Fabry-Perot is that it automatically rejects all Doppler up-shifted, or “anti-Stokes,” spectral components arising from the motion of the moving mirror towards the laser in Figure 2. Such undesirable “anti-Stokes,” or up-shifted, frequency components of the light can rob energy away from the desired “Stokes,” down-shifted, frequency components, specifically, the “idler” frequency necessary for exponential parametric gain to occur. Since the spectral doublet structure of Figure 3(b) does not have any resonance at the “anti-Stokes” frequency, the “Double” Fabry-Perot will serve as a spectral rejection filter that prevents light from building up inside the resonator at any unwanted, Doppler up-shifted frequencies.

#### IV. PELLICLE-MIRROR FABRY-PEROT SYSTEM

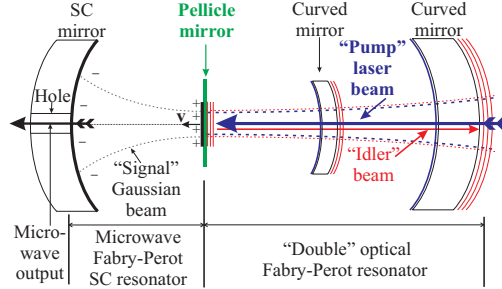


FIG. 4: Pellicle-mirror parametric oscillator for generating microwaves. A thin, charged SC niobium film (in black) is sputtered onto the left side of a thin pellicle substrate (in green). A thin, oppositely charged SC niobium film (also in black) is sputtered onto the reflecting surface of the leftmost curved SC mirror, in order to form an extremely high-Q SC resonator. Optical coatings (in red) are evaporated onto the right side of the pellicle mirror. Thus the pellicle mirror divides the entire structure into two halves. In the left half, the microwave-frequency Fabry-Perot resonator is for resonating a microwave “signal” within a Gaussian beam (in dotted black). In the right half, the “Double” optical Fabry-Perot resonator is for resonating both the “idler” light beam (in dashed red) and the blue-detuned “pump” laser beam (in dashed blue). The microwave mode on the left side of the pellicle is the  $TM_{011}$  mode, and the optical mode on the right side of the pellicle is the  $TEM_{00n}$  mode.

A practical implementation of the “moving mirror” idea at the heart of the microwave parametric oscillator, is to evaporate a thin SC film onto a thin, flexible, low-mass pellicle (with a thickness of around two microns [4]) stretched tautly over a circular wire frame in order to form a “drumhead” with a low-frequency acoustical eigenmode whose mode pattern has a central maximum at the

center of the pellicle. On the reverse side of the pellicle, one could then evaporate dielectric optical coatings to reflect both the strong “pump” laser light beam, and the weak “idler” light beam, for implementing the “Double” Fabry-Perot cavity for the “pump” and “idler” optical beams, which is sketched in Figure 3.

In Figure 4 (which is not drawn to scale, since the diffraction of the microwave-frequency “signal” Gaussian beam will occur much more quickly than the diffraction of the optical-frequency pump and idler light beams), we put together all the pieces of the parametric oscillator system based on the “pellicle mirror” idea. Since microwave frequencies are very much higher than the acoustical frequencies of the pellicle drumhead, the motion of the central portion of the pellicle is essentially like that of a free body (i.e., a free mass) being driven at microwave frequencies.

One can understand the parametric amplification arising in this configuration as follows: When the “pump” laser beam enters from the right into the “Double” optical Fabry-Perot system, the pellicle will act as if it were a piston that is being driven by the radiation pressure force which is varying at the beat note frequency between the strong “pump” laser beam (in blue), whose frequency is  $\omega_p$ , and the weak “idler” (or “Stokes”) beam (in red), whose frequency is  $\omega_i$ , such that this beat note frequency equals the “signal” frequency  $\omega_s$ , which is the  $\text{TM}_{011}$  eigenmode resonance frequency of the left-hand-side microwave Fabry-Perot resonator. Then during the parametric amplification process, one quantum of the pump wave will break up into one quantum of the signal wave plus one quantum of the idler of wave, satisfying the energy conservation relationship

$$\hbar\omega_p = \hbar\omega_i + \hbar\omega_s \quad (3)$$

where  $\hbar\omega_p$  is one quantum of energy of the “pump” mode,  $\hbar\omega_i$  is one quantum of energy of the “idler” mode, and  $\hbar\omega_s$  is one quantum of energy of the “signal” mode.

The moving SC pellicle mirror, when it is viewed as if it were a moving piston, will do work on the “seed” microwaves contained inside the left Fabry-Perot as it moves nonadiabatically [5]. Hence the action of the moving pellicle will amplify this “seed” radiation, which will in turn amplify the motion of the pellicle when it is viewed as a moving optical mirror, because this motion will further amplify the strength of the “Stokes” Doppler sideband of the incoming “pump” laser beam, thus amplifying the strength of the “idler” beam. This in turn increases the strength of the beat note in the radiation pressure force acting on the pellicle, which further increases the amplitude of the motion of the pellicle, etc., in a feedback process. In this way, there will be a mutual reinforcement of the “signal” wave and the “idler” wave, so that an exponential growth of both waves (above a

certain threshold of oscillation) will result, as in a traditional laser. For each quantum produced in the “idler” mode, a quantum of the “signal” mode will be produced as well, in agreement with the Manley-Rowe relations [6].

## V. THRESHOLD FOR PARAMETRIC AMPLIFICATION

We make a simple argument to estimate the threshold for parametric amplification of the pellicle mirror parametric oscillator shown in Figure 4. Let us assume that the microwave cavity on the left side of the parametric amplifier can be modeled as a mirror with a spring attached to a fixed wall (see Figure 2) so that it forms a simple harmonic oscillator with resonant frequency  $\omega_s$ , effective mass  $m$ , and quality factor  $Q_s$ . The right half of the parametric oscillator is regarded as a “Double” optical Fabry-Perot resonator with two resonances at  $\omega_i$  and  $\omega_p$ . The transmission of this “Double” Fabry-Perot has been studied in [7, 8] and is illustrated in Figure 5. Note that the splitting between the double peaks depends on the values of the reflection coefficients. We require that  $r_1 = r_3 \equiv r$  and  $r_2 < r$ , where  $r$  corresponds to reflection coefficient of the two end mirrors, and  $r_2$  to the middle mirror in Figure 3(a). Furthermore, the purpose of the “Double” Fabry-Perot is to allow for the selection of the two desired optical modes  $\omega_i$  and  $\omega_p$ , as already discussed. Since the “Double” Fabry-Perot acts as a single Fabry-Perot with two closely spaced resonances, we treat the parametric amplifier as a single Fabry-Perot cavity with a harmonically moving end mirror as illustrated in Figure 2.

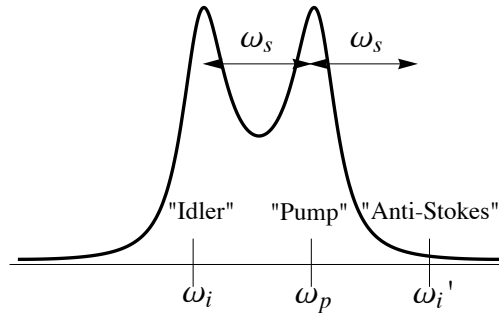


FIG. 5: The transmission of a “Double” Fabry-Perot has resonances at the “idler” mode  $\omega_i$  and the “pump” mode  $\omega_p$ . The difference frequency between “pump” and “idler” is resonant with the “signal” frequency (i.e.,  $\omega_p - \omega_i = \omega_s$ ). The “anti-Stokes”  $\omega_i'$  is off resonance and, hence suppressed.

The Fabry-Perot with a harmonically moving end-mirror (see Appendix C) yields the following



equations of motion

$$\frac{dX}{dt} + \gamma_s X = \frac{i\epsilon_0 \mathcal{A}}{2\omega_s m} \mathcal{E}_{0i}^* \mathcal{E}_{0p} e^{-i\Delta\omega t} \quad (4)$$

$$\frac{d\mathcal{E}_{0i}}{dt} + \gamma_i \mathcal{E}_{0i} = \frac{i}{\tau} X^* \mathcal{E}_{0p} e^{-i\Delta\omega t} \quad (5)$$

where  $\Delta\omega \equiv \omega_p - \omega_i - \omega_s$ ,  $\mathcal{A}$  is the cross sectional area of the resonator,  $X$  is a slowly varying oscillator amplitude,  $\tau$  is the round trip time between the two mirrors of Figure 2,  $\mathcal{E}_{0i}$  is the slowly varying amplitude of the “idler” mode, and  $\gamma_i$ ,  $\gamma_s$  are the HWHM for the “idler” and “signal”, respectively. The problem of a Fabry-Perot with a harmonically moving end-mirror has been solved in detail by [9]. Choosing the same normalization (see Appendix C) as in [9], we arrive at the same results

$$\frac{dX}{dt} + \gamma_s X = \frac{i\omega_p \omega_i}{m\omega_s L} D_p D_i^* e^{-i\Delta\omega t} \quad (6)$$

$$\frac{dD_i}{dt} + \gamma_i D_i = \frac{i\omega_p}{L} X^* D_p e^{-i\Delta\omega t} \quad (7)$$

where  $D_i \propto \mathcal{E}_{0i}$  and  $D_p \propto \mathcal{E}_{0p}$ , and  $L$  is the length of the Fabry-Perot resonator of Figure 2. It was shown in [9] that parametric amplification at resonance occurs if

$$\frac{2U_p Q_i Q_s}{mL^2 \omega_s^2} > 1 \quad (8)$$

where  $U_p$  is the energy stored in the “pump” mode, and the  $Q_i$  and  $Q_s$  are the quality factors of the “idler” and “signal” modes, respectively. We can express this in terms of the outside laser power of the “pump” beam ( $\mathcal{P}_{\text{outside}}$ ) by noting the circulating power inside ( $\mathcal{P}_{\text{inside}}$ ) the Fabry-Perot cavity for the “pump” mode is to a good approximation

$$\mathcal{P}_{\text{inside}} = \frac{\mathcal{F}}{\pi} \mathcal{P}_{\text{outside}} \quad (9)$$

where  $\mathcal{F}$  is the finesse of the Fabry-Perot resonator, assuming a high reflection coefficient for its mirrors. Solving for the outside “pump” intensity gives the threshold condition for parametric amplification

$$\mathcal{P}_{\text{threshold}} = \frac{\pi c}{2\mathcal{F}} \frac{mL\omega_s^2}{Q_i Q_s} \quad (10)$$

where  $L$  is the length of the Fabry-Perot, and  $c$  is the speed of light. For estimates of the threshold we select a reflection coefficient [10]  $r = 0.9999$  for the two end mirrors, and  $r_2 = 0.5$  for the middle mirror (M2 of Figure 3). These values yield a spacing between the two peaks in Figure 5 of  $f_s \approx 10$

GHz, which also corresponds to a finesse of  $\mathcal{F} \approx 15700$ , a  $Q_i \approx 4.5 \times 10^8$  for a 700 nm wavelength; the quality factor of the “signal” is assumed [11–13] to be  $Q_s \sim 10^{10}$ ,  $L = 1$  cm, and  $m$  is assumed to be a free mass [14] on the order of  $m = 2$  mg. With these parameters we find a laser power threshold of

$$\mathcal{P}_{\text{threshold}} = 530 \text{ mW} \quad (11)$$

It is strongly noted that these estimates are based on the ideal model described above. However, it suffices as an order of magnitude estimate and shows that parametric amplification in such a scheme may be possible. Furthermore, parametric amplification of acoustic modes has already been experimentally observed within Fabry-Perot cavities [15, 16].

## VI. THE CASE OF AN ALL-MICROWAVE, ALL-SUPERCONDUCTING RESONATOR SYSTEM

Now suppose that one were to replace the optical “Double” Fabry-Perot system in Figure 4 by a microwave “Double” all-superconducting Fabry-Perot system, so that the entire system becomes an all-microwave, all-superconducting resonator system. Let us also replace the incoming laser “pump” beam by an incoming microwave “pump” beam coming in from the right, and let us then recalculate the pump threshold power needed for parametric oscillation. For the case of microwave resonators having lengths comparable to the microwave wavelength, the cavity finesse  $\mathcal{F}$  becomes comparable to the quality factor  $Q_p$  for the “pump” resonator, so that now the estimate for the threshold power becomes

$$\mathcal{P}_{\text{threshold}}|_{\text{pump}}^{\text{microwave}} \simeq c \frac{mL\omega_s^2}{Q_p Q_i Q_s} \quad (12)$$

Since the system is now an all-superconducting system, we shall assume that [11–13]

$$Q_p \approx Q_i \approx Q_s \approx 10^{10} \quad (13)$$

Again let us assume a mass  $m$  of the pellicle mirror to be 2 mg, and a length  $L$  of the resonator to be 1 cm, which corresponds to a “signal” frequency  $\omega_s$  of  $2\pi \times 15$  GHz, and a “pump” frequency  $\omega_p$  of  $2\pi \times 30$  GHz, in the case of a degenerate parametric oscillator for which  $\omega_s = \omega_i = \omega_p/2$ . One concludes from (12) that

$$\mathcal{P}_{\text{threshold}}|_{\text{pump}}^{\text{microwave}} \simeq 0.05 \text{ } \mu\text{W} \quad (14)$$

Therefore only microwatt-scale “pump” threshold powers are needed for parametric oscillation for an all-microwave, all-superconducting resonator system. This is clearly a feasible experiment to perform.

## VII. APPENDIX A: GAUSSIAN MODE OF A SC HEMICONFOCAL RESONATOR WITH LONGITUDINAL ELECTRIC FIELDS

Here we examine in detail the properties of the fundamental Gaussian-beam mode of the electromagnetic hemiconfocal resonator sketched in Figure 1, following the methodology of the analysis of Ince-Gaussian beams introduced in reference [17].

In order to satisfy the conducting boundary conditions at the SC surface of the flat mirror located at  $z = 0$  in Figure 1, we seek solutions of the vectorized paraxial wave equation [18] which result in a longitudinal electric field vector  $\mathbf{E}_{\text{long}}$  satisfying the conducting boundary conditions at the surface of this mirror, which in turn leads to a *longitudinal* component of the electrical force on the charges located at the surface of the mirror.

The analysis begins with the Maxwell’s equations for electromagnetic fields *in vacuo* [19]

$$\nabla \times \mathbf{E} = -\frac{\partial \mathbf{B}}{\partial t} \quad (15)$$

$$\nabla \times \mathbf{B} = +\mu_0 \varepsilon_0 \frac{\partial \mathbf{E}}{\partial t} \quad (16)$$

$$\nabla \cdot \mathbf{B} = 0 \quad (17)$$

$$\nabla \cdot \mathbf{E} = 0 \quad (18)$$

Assuming that all fields have the same complex exponential time dependence  $\exp(-i\omega t)$  these equations become

$$\nabla \times \mathbf{E} = +i\omega \mathbf{B} \quad (19)$$

$$\nabla \times \mathbf{B} = -i\omega \mu_0 \varepsilon_0 \mathbf{E} \quad (20)$$

$$\nabla \cdot \mathbf{B} = 0 \quad (21)$$

$$\nabla \cdot \mathbf{E} = 0 \quad (22)$$

Taking the curl of the first Maxwell equation (19), and using the second Maxwell equation (20), one gets

$$\nabla \times (\nabla \times \mathbf{E}) = +i\omega (\nabla \times \mathbf{B}) = \omega^2 \mu_0 \varepsilon_0 \mathbf{E} \quad (23)$$

Using the vector identity

$$\nabla \times (\nabla \times \mathbf{E}) = \nabla (\nabla \cdot \mathbf{E}) - \nabla^2 \mathbf{E} \quad (24)$$

and using the fact that in the vacuum,  $\nabla \cdot \mathbf{E} = 0$  (i.e., that there are no charges present within the volume of the resonator), one arrives at the Helmholtz equation for the electric field

$$\nabla^2 \mathbf{E} + \omega^2 \mu_0 \varepsilon_0 \mathbf{E} = \nabla^2 \mathbf{E} + k^2 \mathbf{E} = 0 \quad (25)$$

where

$$k = \omega \sqrt{\mu_0 \varepsilon_0} = \omega/c \quad (26)$$

is the vacuum wavenumber of the EM wave inside the Fabry-Perot resonator shown in Figure 1, with  $c = 1/\sqrt{\mu_0 \varepsilon_0}$  being the vacuum speed of light.

Likewise, one arrives at the Helmholtz equation for the magnetic field

$$\nabla^2 \mathbf{B} + \omega^2 \mu_0 \varepsilon_0 \mathbf{B} = \nabla^2 \mathbf{B} + k^2 \mathbf{B} = 0 \quad (27)$$

Note that the Fabry-Perot resonator configuration of Figure 1 has a dominant axis of propagation, namely, the  $z$  axis. This suggests that a paraxial wave approximation for the  $z$  component of the electric field might be useful here.

An important reason for singling out the  $z$  component of the electric field for the Helmholtz equation is that the boundary conditions at the flat SC mirror require that the longitudinal (or normal) component of the electric field does not vanish at the surface of the mirror, but that the transverse (or tangential) components of the electric field must vanish at this conducting (or superconducting) boundary. This boundary condition singles out a transverse magnetic mode as the fundamental mode of the resonator.

Let us choose the surface of the flat mirror to coincide with the  $z = 0$  plane. Then from the above conducting boundary conditions, we expect that the longitudinal component  $E_z$  is a

maximum at  $z = 0$ , and also at  $z = -L$  at the conducting surface of the curved mirror, but that the transverse components of the electric field vanish at these surfaces. We therefore seek solutions of the  $z$  component of the the electric field from Helmholtz equation (25), i.e.,

$$\nabla^2 E_z + k^2 E_z = 0 \quad (28)$$

that satisfy these boundary conditions. From these solutions for  $E_z$ , we can derive the transverse components of the electric and magnetic fields of the modes of the resonator, in a procedure similar to finding the fields of the transverse magnetic (TM) modes of a microwave resonator [19]. In other words, the conducting boundary conditions for the configuration of mirrors shown in Figure 1 demand that the  $z$  component of the magnetic field must be zero everywhere on the surfaces of the mirrors, i.e.,

$$B_z = 0 \quad (29)$$

a condition that is also required by the Meissner effect in SC's.

It is then natural to try as a solution of the Helmholtz equation (28) the following *Ansatz* for the  $z$  component of the electric field:

$$E_z(x, y, z, t) = E_0 \psi(x, y, z) \cos kz \exp(-i\omega t) + c.c. \quad (30)$$

where  $E_0$  is a constant,  $\psi(x, y, z)$  is a dimensionless factor with a complex amplitude that varies slowly with  $z$  compared to the fast  $z$  dependence of the factor  $\cos kz$ , and “c.c.,” as usual, is the complex conjugate of the previous term. We have chosen here the  $z$  dependence to be that of a cosine rather than a sine function in order to satisfy the boundary condition that  $E_z$  is maximum (i.e., an anti-node) at  $z = 0$ . This leads to a standing-wave solution for the mode of the SC resonator.

Therefore neglecting the second derivative of  $\psi(x, y, z)$  with respect to  $z$ , which is assumed to be small compared to the first derivative with respect to  $z$ , we arrive at the paraxial wave equation for the slowly varying amplitude  $\psi$

$$2ik \frac{\partial \psi}{\partial z} + \nabla_t^2 \psi = 0 \quad (31)$$

where the transverse Laplacian  $\nabla_t^2$  is

$$\nabla_t^2 = \frac{\partial^2}{\partial x^2} + \frac{\partial^2}{\partial y^2} \quad (32)$$

Note that the paraxial wave equation (31) has the same mathematical form as the time-dependent Schrödinger equation

$$\frac{\hbar}{i} \frac{\partial \psi}{\partial t} = -\frac{\hbar^2}{2m} \nabla^2 \psi \quad (33)$$

except that the axial distance  $z$  in the paraxial resonator problem has now been replaced by the time  $t$  in the quantum mechanics problem. Since we know that spreading Gaussian wavepacket solutions are solutions to the time-dependent Schrödinger equation (33), we expect that analogous Gaussian solutions will also be solutions to the paraxial wave equation (31).

For the Fabry-Perot resonator configuration of Figure 1, the procedure is to first solve the paraxial wave equation (31) for  $E_z$  after setting  $B_z = 0$  everywhere. Then one substitutes these solutions into the right-hand sides of Maxwell's equations as source terms to obtain solutions for the transverse fields  $E_x$  and  $E_y$ .

The lowest-order Gaussian solution to the paraxial wave equation (31) can be obtained starting from the following ‘‘Gaussian’’ *Ansatz*:

$$\psi(x, y, z) = \Psi_G(x, y, z) = \exp i \left( P(z) + \frac{1}{2} Q(z) r^2 \right) \quad (34)$$

where  $P(z)$  and  $Q(z)$  are complex functions of the axial distance  $z$ , and where

$$r^2 = x^2 + y^2 \quad (35)$$

is the square of the radial distance  $r$  of a field point displaced away from the axis of the resonator. Note that  $r$  is a real variable.

It follows from this Gaussian *Ansatz* that

$$\frac{\partial^2}{\partial x^2} \Psi_G = iQ \Psi_G - Q^2 x^2 \Psi_G \quad (36)$$

$$\frac{\partial^2}{\partial y^2} \Psi_G = iQ \Psi_G - Q^2 y^2 \Psi_G \quad (37)$$

so that the paraxial wave equation, which is a PDE, reduces to the ODE

$$-2k \frac{dP}{dz} - 2k \cdot \frac{1}{2} \frac{dQ}{dz} r^2 + 2iQ - Q^2 r^2 = 0 \quad (38)$$

Collecting the coefficients of  $r^2$  in this equation and setting their sum equal to zero, one then arrives at the two first-order ODE's

$$k \frac{dQ}{dz} + Q^2 = 0 \quad (39)$$

$$-k \frac{dP}{dz} + iQ = 0 \quad (40)$$

The solution of (39) can be obtained by integration as follows:

$$\int \frac{dQ}{Q^2} + \frac{1}{k} \int dz = 0 \quad (41)$$

Transforming variables using

$$Q = \frac{1}{q} \quad (42)$$

one finds that (41) becomes

$$- \int_{q_0}^{q(z)} dq + \frac{1}{k} \int_0^z dz = 0 \quad (43)$$

and therefore that the solution to the ODE for  $Q$  (39) can be rewritten as follows:

$$q(z) - q_0 = \frac{1}{k}z \quad (44)$$

It should be kept in mind that since  $Q(z)$  is a complex function of  $z$ , so likewise  $q(z)$  will also be a complex function of  $z$ .

In analogy with the Gaussian wavepacket-spreading problem in quantum mechanics, it is natural to impose on the Gaussian *Ansatz* (34) as an initial condition (i.e., boundary condition) at  $z = 0$ , that it reduces to the *real* Gaussian function

$$\begin{aligned} \Psi_G(x, y, 0) &= \exp i \left( P(0) + \frac{1}{2}Q(0)r^2 \right) \\ &= \exp(-r^2/w_0^2) \end{aligned} \quad (45)$$

where the real number  $w_0$  is the initial Gaussian wavepacket size evaluated at the  $z = 0$  plane, which corresponds to the “beam waist” size at the flat mirror in Figure 1. Then

$$q_0 = \frac{1}{Q(0)} = -\frac{i}{2}w_0^2 \quad (46)$$

is determined to be an imaginary number. Also, it then follows from the initial condition (45) that the initial value of  $P(z)$  must be

$$P(0) = 0 \quad (47)$$

Therefore the solution for  $q(z)$  (44) becomes

$$q(z) = q_0 + \frac{z}{k} = -\frac{i}{2}w_0^2 + \frac{z}{k} = \frac{z - ikw_0^2/2}{k} = \frac{z - iz_R}{k} \quad (48)$$

where the ‘‘Rayleigh range’’  $z_R$  is defined as follows:

$$z_R = kw_0^2/2 \quad (49)$$

The meaning of the Rayleigh range  $z_R$  is that it is the distance scale on which the width of the Gaussian beam will have significantly increased due to diffraction (i.e., wavepacket spreading due to the uncertainty principle). The paraxial approximation holds when diffraction angle  $\theta_{\text{diffraction}}$  due to the spreading of the Gaussian beam is sufficiently small, i.e., when

$$\theta_{\text{diffraction}} \simeq \frac{\lambda}{w_0} < 1 \quad (50)$$

Therefore the paraxial approximation is satisfied when the Rayleigh range satisfies the condition

$$z_R = kw_0^2/2 = \pi w_0^2/\lambda \simeq \pi\lambda/\theta_{\text{diffraction}}^2 \geq \lambda/2 \quad (51)$$

Transforming back from the function  $q(z)$  to the original function  $Q(z)$ , one finds from (48) that

$$\begin{aligned} Q(z) &= \frac{1}{q(z)} = k \left( \frac{1}{z - iz_R} \right) = k \left( \frac{z + iz_R}{z^2 + z_R^2} \right) \\ &= k \left( \frac{1}{z + z_R^2/z} + i \frac{z_R}{z^2 + z_R^2} \right) \end{aligned} \quad (52)$$

It therefore follows that in the Gaussian *Ansatz* (34), the exponential factor  $\exp\left(\frac{i}{2}Q(z)r^2\right)$  can be factorized as follows:

$$\begin{aligned} \exp\left(\frac{i}{2}Q(z)r^2\right) &= \exp\left(\frac{i}{2} \frac{kr^2}{z + z_R^2/z}\right) \\ &\times \exp\left(-\frac{1}{2} \frac{kr^2}{(1 + z^2/z_R^2)z_R}\right) \\ &= \exp\left(\frac{i}{2} \frac{kr^2}{R(z)}\right) \exp\left(-\frac{r^2}{w^2(z)}\right) \end{aligned} \quad (53)$$

where

$$R(z) = z + z_R^2/z \quad (54)$$

is the radius of curvature of the phasefront of  $\Psi_G(x, y, z)$  at  $z$ , and where

$$w^2(z) = w_0^2 \left( 1 + \frac{z^2}{z_R^2} \right) \quad (55)$$



is the square of the spreading Gaussian beam width at  $z$ . Thus one concludes that the area of the Gaussian beam, as measured by  $w^2(z)$  evaluated at  $z = z_R$ , will double due to diffraction from its initial value  $w_0^2$  evaluated at the  $z = 0$  plane.

Next, we shall find the solution of the ODE (40) for  $P(z)$ , starting from the known solution (52) for  $Q(z)$ , by direct integration, as follows:

$$\begin{aligned} P(z) &= \frac{i}{k} \int_0^z Q(z) dz = i \int_0^z \frac{1}{z - iz_R} dz \\ &= i \ln \left( \frac{z - iz_R}{-iz_R} \right) \end{aligned} \quad (56)$$

Therefore it follows that the first exponential factor in the Gaussian *Ansatz* (34) can be expressed as

$$\begin{aligned} &\exp(iP(z)) \\ &= \exp \left( -\ln \left[ \left( \frac{\sqrt{z^2 + z_R^2}}{z_R} \right) \exp(i\varphi_G(z)) \right] \right) \\ &= \frac{1}{\sqrt{1 + z^2/z_R^2}} \exp \left( -i \arctan \frac{z}{z_R} \right) \end{aligned} \quad (57)$$

where

$$\varphi_G(z) = -\arctan \frac{z}{z_R} \quad (58)$$

is called the ‘‘Gouy phase shift’’.

Putting everything together, one then finds that the Gaussian *Ansatz* (34) becomes

$$\begin{aligned} \Psi_G(x, y, z) &= \frac{w_0}{w(z)} \exp \left( -\frac{r^2}{w^2(z)} \right) \\ &\quad \times \exp \left\{ i \frac{kr^2}{2R(z)} - i \arctan \frac{z}{z_R} \right\} \end{aligned} \quad (59)$$

which is a solution of the paraxial wave equation

$$2ik \frac{\partial \Psi_G}{\partial z} + \frac{\partial^2 \Psi_G}{\partial x^2} + \frac{\partial^2 \Psi_G}{\partial y^2} = 0 \quad (60)$$

and that therefore the full standing-wave solution for the longitudinal electric field in the transverse-

magnetic  $\text{TM}_{01n}$  mode of the SC resonator becomes

$$\begin{aligned}
E_z(x, y, z, t) &= E_0 \Psi_G \cos kz \exp(-i\omega t) + \text{c.c.} \\
&= E_0 \frac{w_0}{w(z)} \exp\left(-\frac{r^2}{w^2(z)}\right) \\
&\quad \times \exp\left\{i\frac{kr^2}{2R(z)} - i \arctan \frac{z}{z_R}\right\} \\
&\quad \times \cos kz \exp(-i\omega t) + \text{c.c.}
\end{aligned} \tag{61}$$

The first boundary condition at the flat mirror at  $z = 0$  will be satisfied, since

$$\cos kz = 1 \text{ at } z = 0 \tag{62}$$

and therefore at  $z = 0$

$$E_z(x, y, 0, t) = E_0 \exp\left(-\frac{r^2}{w_0^2}\right) \exp(-i\omega t) + \text{c.c.} \tag{63}$$

i.e., that the longitudinal electric field has a standing-wave anti-node at  $z = 0$ . If one further assumes that the curvature of the curved mirror in Figure 1 matches the curvature of the curved phase front  $R(z)$  given by (54) evaluated at  $z = -L$ , then the second boundary condition at the curved mirror at  $z = -L$  will be satisfied when

$$\cos kL = \pm 1 \text{ for } kL = n\pi \text{ where } n = 1, 2, 3, \dots \tag{64}$$

i.e., that the longitudinal electric field has a standing-wave anti-node at  $z = -L$  (we neglect here a small correction factor arising from the Gouy phase shift). Therefore the standing-wave anti-node condition (64) determines the  $\text{TM}_{01n}$  eigenmode frequencies of the SC resonator depicted in Figure 1 through the relationship

$$\omega_n = ck_n = 2\pi \cdot n \frac{c}{2L} \text{ where } n = 1, 2, 3, \dots \tag{65}$$

Hence the fundamental eigenmode, i.e., the one with the lowest resonance frequency, corresponds to the mode number  $n = 1$ , i.e., the  $\text{TM}_{011}$  mode.

In order to find the transverse components  $E_x(x, y, z, t)$  and  $E_y(x, y, z, t)$ , let us return to Maxwell's equations. Since no free charges are present in the vacuum between the two SC mirrors of Figure 1, it follows that  $\nabla \cdot \mathbf{E} = 0$ , and therefore that

$$\frac{\partial E_x}{\partial x} + \frac{\partial E_y}{\partial y} = -\frac{\partial E_z}{\partial z} \tag{66}$$

From the paraxial approximation condition (51), one concludes that the leading term on the right-hand side will be given by

$$-\frac{\partial E_z}{\partial z} \doteq E_0 \Psi_G(x, y, z) k \sin kz \exp(-i\omega t) + \text{c.c.} \quad (67)$$

This suggests that we try as trial solutions

$$E_x = x \cdot \frac{E_0}{2} \Psi_G k \sin kz \exp(-i\omega t) + \text{c.c.} \quad (68)$$

$$E_y = y \cdot \frac{E_0}{2} \Psi_G k \sin kz \exp(-i\omega t) + \text{c.c.} \quad (69)$$

because then

$$\frac{\partial(x\Psi_G)}{\partial x} = \Psi_G + x \frac{\partial\Psi_G}{\partial x} = \Psi_G + x \frac{i}{2} Q \cdot x\Psi_G \quad (70)$$

where the last term can be neglected in the paraxial approximation, so that the leading terms are

$$\frac{\partial(x\Psi_G)}{\partial x} \doteq \Psi_G \quad (71)$$

$$\frac{\partial(y\Psi_G)}{\partial y} \doteq \Psi_G \quad (72)$$

Therefore (66) becomes

$$\frac{1}{2}k \frac{\partial(x\Psi_G)}{\partial x} + \frac{1}{2}k \frac{\partial(y\Psi_G)}{\partial y} \doteq k\Psi_G \quad (73)$$

which holds true in the paraxial approximation.

As a further check of the validity of the above trial solutions (68) and (69), let us verify that Faraday's law in component form

$$\frac{\partial E_x}{\partial y} - \frac{\partial E_y}{\partial x} = -\frac{\partial B_z}{\partial t} = 0 \quad (74)$$

is satisfied. One finds that

$$\frac{\partial E_x}{\partial y} \propto \frac{\partial(x\Psi_G)}{\partial y} = x \cdot 2y \cdot iQ\Psi_G \quad (75)$$

$$\frac{\partial E_y}{\partial x} \propto \frac{\partial(y\Psi_G)}{\partial x} = y \cdot 2x \cdot iQ\Psi_G \quad (76)$$

cancel each other, so that we see that (74) is indeed satisfied. We therefore conclude that, in the paraxial approximation, (68) and (69) are indeed the unique solutions for the transverse components  $E_x$  and  $E_y$  that correspond to the paraxial  $\text{TM}_{01n}$  Gaussian-beam solution  $E_z$  given by (61).

The two transverse magnetic field components  $B_x$  and  $B_y$  can then be gotten from the two Maxwell equations

$$\frac{\partial B_x}{\partial x} + \frac{\partial B_y}{\partial y} = -\frac{\partial B_z}{\partial z} = 0 \quad (77)$$

$$\frac{\partial B_x}{\partial y} - \frac{\partial B_y}{\partial x} = \mu_0 \varepsilon_0 \frac{\partial E_z}{\partial t} = -i\omega \mu_0 \varepsilon_0 E_z \quad (78)$$

By inspection, the solutions for  $B_x$  and  $B_y$  of (77) and (78) are

$$B_x = y \cdot \frac{E_0}{2c} \Psi_G k \cos kz (-ie^{-i\omega t}) + \text{c.c.} \quad (79)$$

$$B_y = -x \cdot \frac{E_0}{2c} \Psi_G k \cos kz (-ie^{-i\omega t}) + \text{c.c.} \quad (80)$$

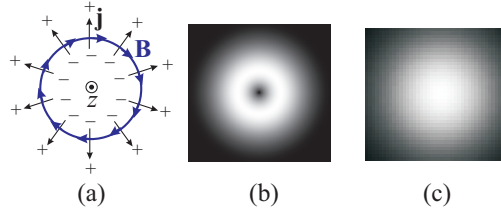


FIG. 6: (a) Sketch of a snapshot of the pattern of supercurrents  $\mathbf{j}$  (black arrows) flowing on the surface of the SC flat mirror at  $z = 0$  of Figure 1, and their associated magnetic field vectors  $\mathbf{B}$  (blue arrows) immediately outside of the SC surface. This pattern of currents and fields is associated with the circularly symmetric  $\text{TM}_{01n}$  mode solution (61). (b) Transverse intensity profile of this mode (i.e., the sum of the absolute squares of  $E_x$  and  $E_y$  given by (68) and (69), respectively). (c) Longitudinal intensity profile (i.e., the absolute square of  $E_z$  given by (61)).

The above solutions can be depicted as the circularly symmetric, transverse magnetic  $\text{TM}_{01n}$  mode pattern sketched in Figure 6(a), which is a snapshot taken looking down the  $z$  axis of the hemiconfocal resonator at the  $z = 0$  plane of the flat SC mirror of Figure 1, at the moment of maximum magnetic field. In Figure 6(b), the transverse intensity pattern of this mode is depicted. The circular symmetry of this pattern can be readily understood by taking the absolute square of the transverse electric fields of this mode, which are given by (68) and (69), i.e.,

$$E_x \propto x = r \cos \theta \quad (81)$$

$$E_y \propto y = r \sin \theta \quad (82)$$

so that

$$|E_x|^2 + |E_y|^2 \propto r^2 \quad (83)$$

which is clearly independent of the azimuthal angle  $\theta$ . Figure 6(c) shows the longitudinal intensity profile of  $|E_z|^2$ .

### VIII. APPENDIX B: SIMPLE HARMONIC OSCILLATOR MODEL FOR THE MICROWAVE CAVITY-PELLICLE MIRROR SYSTEM

Here it is shown that the superconducting (SC) microwave cavity with a pellicle end-mirror (see Figures 1 and 4) can be modeled as a simple harmonic oscillator whose loaded quality factor  $Q_{\text{loaded}}$  is approximately given by the quality factor of the SC cavity  $Q_s$ .

Let the pellicle end-mirror consist of a thin SC film deposited on a thin, light, flexible diaphragm, which is sufficiently thin so that it can easily be driven into mechanical motion. Furthermore, suppose that the SC film is electrostatically charged with a net DC charge  $q$ . We assume that the charge  $q$  which resides on the surface of the film is so tightly bound (via the Coulomb force) to the metallic film that when the charge  $q$  moves, the film will co-move with it [20]. Then the longitudinal electric field  $\mathbf{E}_z$  at the surface of the SC film will lead to the instantaneous force

$$\mathbf{F}_z(t) = q\mathbf{E}_z(t) + \mathbf{F}_{\text{rad}}(t) \quad (84)$$

where  $\mathbf{E}_z$  is the longitudinal electric field at the surface of the SC film, and where the force on the film due to radiation pressure is given by

$$\mathbf{F}_{\text{rad}}(t) = \frac{1}{2}\epsilon_0\mathbf{E}_z(t)^2\mathcal{A} \propto \mathbf{E}_z(t)^2 \quad (85)$$

where  $\epsilon_0$  is the permittivity of free space, and  $\mathcal{A}$  is the area of the film over which  $\mathbf{E}_z(t)$  is nonvanishing, i.e., the Gaussian-beam-waist area of Figure 6(c). Since the radiation force  $\mathbf{F}_{\text{rad}}(t)$  scales quadratically with the electric field at the surface of the film, while the Coulomb force  $q\mathbf{E}_z(t)$  scales linearly, there exists a maximum electric field strength  $E_{\text{max}}$  such that if  $|E_z(t)| < E_{\text{max}}$ , then the Coulomb force  $q\mathbf{E}_z(t)$  dominates over the radiation force  $\mathbf{F}_{\text{rad}}(t)$ . Comparing (84) and (85), one finds that

$$E_{\text{max}} = \frac{2q}{\epsilon_0\mathcal{A}}$$

Expressing this condition in terms of a maximum externally applied “seed” power ( $\mathcal{P}_{\text{ext}}^{\text{max}}$ ) and the maximum circulating power in the cavity ( $\mathcal{P}_{\text{cav}}^{\text{max}}$ ) we find

$$\mathcal{P}_{\text{ext}}^{\text{max}} = \frac{U_0\omega}{4Q_s} \approx 7 \text{ nW} \quad (86)$$

$$\mathcal{P}_{\text{cav}}^{\text{max}} = \frac{q^2c}{\epsilon_0\mathcal{A}} \approx 43 \text{ W} \quad (87)$$

where we have assumed perfect coupling between the externally applied “seed” power and the cavity,  $\mathcal{A} = \pi w_0^2$  is the cross-sectional area given by the beam waist (with  $w_0 = 1 \text{ cm}$ ) of the  $\text{TM}_{011}$  mode in cavity,  $q \approx 20 \text{ pC}$  for 100 Volts DC,  $\omega = 2\pi \times 12 \text{ GHz}$ , and  $Q_s = 10^{10}$  [12]. For the rest of this analysis, we assume that we are in the regime where the circulating power in the cavity is sufficiently less than 43 W, or, more generally, that it is less than  $\mathcal{P}_{\text{cav}}^{\text{max}}$ , so that the radiation force is negligible, and (84) becomes

$$\mathbf{F}_z(t) \approx q\mathbf{E}_z(t) \quad (88)$$

At high (i.e., microwave) frequencies we take the approximation that the pellicle end-mirror behaves like a free mass, so that the equation of motion for the pellicle mirror is given as

$$m \frac{d^2x}{dt^2} = qE(t), \quad (89)$$

where we drop the subscript  $z$  from  $\mathbf{E}_z(t)$  for convenience, and we switch from  $z$  to the variable  $x$  to denote the displacement of the oscillating mass  $m$  from equilibrium. The time-dependent part of the longitudinal electric field at the surface of the SC film can be described as a harmonically time-varying field given by

$$E(t) = \mathcal{E}(t)e^{-i\omega t} + \text{c.c.}$$

where  $\mathcal{E}(t)$  is a slow varying amplitude. It follows that the displacement of the charged mirror is given by

$$x(t) = -\frac{q}{m\omega^2}E(t). \quad (90)$$

Observe that the displacement  $x(t)$  is *linear* with the longitudinal electric field  $E(t)$  evaluated at the surface of the flat mirror in the SC resonator. Now suppose that the SC resonator is in steady state and filled with some constant input power from some “seed” microwaves so that the pellicle end-mirror displacement is given by (90). If we then shut off the injected “seed” power, the SC

resonator's electric field will decay exponentially with time. Hence, the displacement of the pellicle end-mirror will also decay exponentially with time. It now suffices to show that the electric field  $E(t)$  in the resonator can be described by a simple harmonic oscillator. The equation of motion for the undriven simple harmonic oscillator is

$$\frac{d^2x}{dt^2} + 2\gamma\frac{dx}{dt} + \omega^2x = 0 \quad (91)$$

where  $\gamma$  is the decay parameter of the oscillator. Using (90) we arrive at an equivalent simple harmonic motion equation for the field in the cavity

$$\frac{d^2E}{dt^2} + 2\gamma\frac{dE}{dt} + \omega^2E = 0 \quad (92)$$

where  $E$  is the electric field evaluated at the surface of the moving mirror, where we interpret  $2\gamma$  as the FWHM of the SC cavity resonance, and where  $\omega$  is the resonance frequency of the SC resonator. (Note that (92) also follows from the Helmholtz analysis for a lossy resonator.) In the slowly varying amplitude approximation, (92) reduces to a first order linear differential equation for the slowly varying amplitude

$$\frac{d\mathcal{E}}{dt} + \gamma\mathcal{E} = 0 \quad (93)$$

whose solution is

$$\mathcal{E}(t) = E_0e^{-\gamma t} = E_0e^{-\omega t/2Q_s} \quad (94)$$

where  $E_0$  is the initial electric field amplitude at the surface of the mirror, and  $Q_s = \omega/2\gamma$  is the SC resonator's intrinsic quality factor. Therefore, the field in the SC microwave resonator decays like a simple harmonic oscillator with a time constant that is proportional to the quality factor of the cavity. Furthermore, since the displacement of the pellicle end-mirror is linear with the field inside the resonator, it must also decay like a simple harmonic oscillator. Note that with (94) we can write the field inside the resonator as

$$E(t) = E_0e^{-\omega t/2Q_s}e^{-i\omega t} + \text{c.c.} \quad (95)$$

which is the well-known exponentially decaying solution with the ringdown time

$$\tau_r = 2Q_s/\omega$$

of the resonator.

Finally we take into consideration the effect that driving the pellicle end-mirror with “seed” radiation has on the quality factor  $Q_s$  of the SC resonator. The loaded quality factor  $Q_{\text{loaded}}$ , where the loading refers to the power loss due to the simple harmonic motion of the charged mirror, is given by

$$Q_{\text{loaded}} = \frac{\omega U_0}{\mathcal{P}_{\text{loss}}} \quad (96)$$

where  $U_0$  is the energy stored in the cavity, and  $\mathcal{P}_{\text{loss}}$  is the total power loss in the cavity given by

$$\mathcal{P}_{\text{loss}} = \mathcal{P}_c + \mathcal{P}_{\text{mirror}} \quad (97)$$

where  $\mathcal{P}_c$  is the intrinsic power loss of the SC resonator and is related to the resonator’s intrinsic quality factor by  $Q_s = \omega U_0 / \mathcal{P}_c$ , and where  $\mathcal{P}_{\text{mirror}}$  is the average power loss due to the motion of the charged pellicle end-mirror. From (96) one finds that

$$Q_{\text{loaded}} = \frac{Q_s Q_{\text{SHM}}}{Q_s + Q_{\text{SHM}}} \quad (98)$$

where  $Q_{\text{SHM}} \equiv \omega U_0 / \mathcal{P}_{\text{mirror}}$  is the contribution to the quality factor arising from simple harmonic motion (SHM). Although it is possible that some or all of the power loss that goes into the simple harmonic motion of the charged mirror is converted into electromagnetic radiation power which goes back into the SC resonator, it is instructive to account for it. The average power loss due to the moving pellicle end-mirror is

$$\mathcal{P}_{\text{mirror}} = \langle \mathbf{F} \cdot \mathbf{v} \rangle = \frac{q^2 E_0^2}{2m\omega}. \quad (99)$$

The electric field is calculated by assuming some externally applied “seed” power  $\mathcal{P}_{\text{ext}}$  is injected into the SC resonator. In steady state, the energy in the cavity  $U_0$  is

$$U_0 = \frac{4\beta \mathcal{P}_{\text{ext}} Q_s}{(1 + \beta)^2 \omega} \quad (100)$$

where  $\beta$  is a coupling parameter of the input/output hole in Figure 1 and is assumed to be unity,  $\beta \equiv 1$ . It follows that the amplitude of the electric field inside the cavity  $E_0$  is given by

$$E_0^2 = \frac{8\mathcal{P}_{\text{ext}} Q_s}{m\omega \mathcal{V} \epsilon_0} \quad (101)$$

where  $\mathcal{V}$  is the effective Gaussian-beam volume of the SC resonator. Hence, the average power loss from the pellicle end-mirror is

$$\mathcal{P}_{\text{mirror}} = \frac{4q^2 \mathcal{P}_{\text{ext}} Q_s}{m\omega^2 \mathcal{V} \epsilon_0}. \quad (102)$$



Assuming an external applied “seed” power of  $\mathcal{P}_{\text{ext}} = 500$  pW,  $q = 20$  pC,  $Q_s = 10^{10}$ ,  $m = 2$  mg,  $\omega = 2\pi \times 12$  GHz, and an effective Gaussian-beam volume of  $\mathcal{V} = 1.25$  cm<sup>3</sup>, one finds

$$\mathcal{P}_{\text{mirror}} \approx 6 \times 10^{-20} \text{ W} \quad (103)$$

This power yields

$$Q_{\text{SHM}} \approx 4 \times 10^{21}. \quad (104)$$

Since  $Q_s \ll Q_{\text{SHM}}$ , it follows from (98) that to an extremely good approximation

$$Q_{\text{loaded}} \approx Q_s$$

### IX. APPENDIX C: SIMPLE SOLUTION TO A FABRY-PEROT WITH A HARMONICALLY MOVING END-MIRROR IN QUASI STEADY STATE

We consider a Fabry-Perot under quasi steady state conditions and ignore transients during the build up of the modes as those discussed in [21]. In a quasi steady state, the harmonically moving end-mirror generates two Doppler side bands, “Stokes” and “anti-Stokes” [22]. The “anti-Stokes” sideband is suppressed via the “Double” Fabry-Perot scheme as illustrated in Figures 3 and 5.

The radiation force is given by

$$F(t) = \frac{1}{2} \epsilon_0 |E|^2 \mathcal{A} \quad (105)$$

where  $\epsilon_0$  is the permittivity of free space,  $\mathcal{A}$  is the cross sectional area of the Gaussian beam, and  $E$  is the total electric field in the Fabry-Perot. Modeling the moving end-mirror as a simple harmonic oscillator as depicted in Figure 2, we have

$$\ddot{x} + 2\gamma_s \dot{x} + \omega_s^2 x = \frac{F(t)}{m}, \quad (106)$$

where  $x$  is the displacement of the simple harmonic oscillator from equilibrium,  $\omega_s$  is the natural oscillator frequency,  $m$  is its mass, and  $2\gamma_s$  is the FWHM. Using the slowly varying amplitude approximation in quasi steady state

$$x = X(t)e^{-i\omega_s t} + \text{c.c.} \quad (107)$$

the left side of (106) becomes

$$-2i\omega_s \left( \frac{dX}{dt} + \gamma_s X \right) e^{-i\omega_s t} + \text{c.c.} \quad (108)$$

where we have assumed that  $2(\gamma_s - i\omega_s) \approx -2i\omega_s$ . The right hand side can be expanded in terms of the fields

$$E_i = \mathcal{E}_{0i}(t)e^{-i\omega_i t} + \text{c.c.}, \quad E_p = \mathcal{E}_{0p}e^{-i\omega_p t} + \text{c.c.} \quad (109)$$

where the former is the ‘‘Stokes’’ or ‘‘idler’’ term and the latter is the ‘‘pump’’ mode,  $\mathcal{E}_{0i}(t)$  being a slowly varying amplitude in quasi steady state, but  $\mathcal{E}_{0p}$  being a constant, in the ‘‘undepleted pump’’ approximation. Taking the beat terms and neglecting the nonresonant terms  $|E_i|^2$  and  $|E_p|^2$  we have

$$\begin{aligned} F(t) = & \epsilon_0 \mathcal{A} [\mathcal{E}_{0i}^* \mathcal{E}_{0p} e^{-i(\omega_p - \omega_i)t} \\ & + \mathcal{E}_{0i} \mathcal{E}_{0p} e^{-i(\omega_p + \omega_i)t} + \text{c.c.}] \end{aligned} \quad (110)$$

Equating both sides and multiplying by  $e^{i\omega_s t}$  we find

$$\begin{aligned} & -2i\omega_s \left( \frac{dX}{dt} + \gamma_s X \right) + \text{c.c.} (\propto e^{2i\omega_s t}) \\ = & \frac{\epsilon_0 \mathcal{A}}{m} [\mathcal{E}_{0i}^* \mathcal{E}_{0p} e^{-i(\omega_p - \omega_i - \omega_s)t} + \mathcal{E}_{0i} \mathcal{E}_{0p} e^{2i\omega_i t} \\ & + \text{c.c.} (\propto e^{i2\omega_s t}, e^{i2\omega_p t})], \end{aligned} \quad (111)$$

where  $\omega_p - \omega_i \approx \omega_s$ . Here we employ the fact that this is a linear system and observe that only the force at resonance will be the main driving force of the mechanical oscillator; hence, we can neglect off-resonance terms (in the rotating-wave approximation), and write the driven oscillator equation as

$$\frac{dX}{dt} + \gamma_s X = \frac{i\epsilon_0 \mathcal{A}}{2\omega_s m} \mathcal{E}_{0i}^* \mathcal{E}_{0p} e^{-i(\omega_p - \omega_i - \omega_s)t} \quad (112)$$

Following [9], let us define the fields as

$$E_i(t) = A_i(D_i(t)e^{-i\omega_i t} + \text{c.c.}) \quad (113)$$

$$E_p = A_p(D_p e^{-i\omega_p t} + \text{c.c.}) \quad (114)$$

where  $A_i$ ,  $A_p$  are normalized so that the total energy stored in each mode is  $U_{p,i} = 2\omega_{p,i}|D_{p,i}|^2$ , and  $D_i(t)$  is a slowly varying complex amplitude, but  $D_p$  is a constant, in the ‘‘undepleted pump’’ approximation. Calculating the energies in each mode we find

$$U_{p,i} = \frac{\mathcal{V}}{2} \epsilon_0 \langle E^2 \rangle = A_{p,i}^2 \epsilon_0 |D_{p,i}|^2 \mathcal{A} L = 2\omega_{p,i}^2 |D_{p,i}|^2 \quad (115)$$

where  $\mathcal{V} = \mathcal{A}L$  is the volume of the cavity. Solving for  $A_{p,i}$

$$A_{p,i} = \omega_{p,i} \sqrt{\frac{2}{\epsilon_0 \mathcal{V}}} \quad (116)$$

Inserting the normalization

$$\mathcal{E}_{0i}^* = A_i D_i^* \text{ and } \mathcal{E}_{0p} = A_p D_p \quad (117)$$

into equation (112) we arrive at the result [9], eq. (2),

$$\frac{dX}{dt} + \gamma_s X = \frac{i\omega_p \omega_i}{m\omega_s L} D_p D_i^* e^{-i\Delta\omega t} \quad (118)$$

where  $\Delta\omega \equiv \omega_p - \omega_i - \omega_s$ .

To arrive at the equation for the ‘‘Stokes’’ or ‘‘idler’’ field in the cavity we note that the ‘‘Stokes’’ mode is generated from the main ‘‘pump’’ mode so that the ‘‘Stokes’’ field is proportional to the oscillator amplitude. Recall that we are assuming quasi steady state conditions. The electric field reflected from a moving mirror is given by [22]

$$E_p = \mathcal{E}_{0p} e^{-i\omega_p t} e^{2ik_p x} + \text{c.c.} \quad (119)$$

For small  $x$ , we find

$$E_p = \mathcal{E}_{0p} e^{-i\omega_p t} (1 + 2ik_p x) + \text{c.c.} \quad (120)$$

where the last term leads to the Doppler-generated electric field

$$E_{\text{Doppler}} \equiv 2ik_p x \mathcal{E}_{0p} e^{-i\omega_p t} + \text{c.c.} \quad (121)$$

Since we assume quasi steady state conditions, the ‘‘pump’’ optical mode is the main source of the ‘‘Stokes’’ optical mode. As is well known, the Fabry-Perot cavity field obeys a recursion relation; for example see [21, 23]. Hence

$$E_i(t + \tau) = E_{\text{Doppler}}(t + \tau) + \mathcal{R}P_f E_i(t) \quad (122)$$

where  $\tau = 2L/c$  is the round trip time,  $\mathcal{R}$  is the power reflectivity (i.e., the absolute square of the reflection coefficient) of the end mirrors,  $P_f$  is a propagation factor [21, 23] which accounts for the phase accumulated by the beam one round trip earlier, and  $E_{\text{Doppler}}$  is the Doppler electric field generated from the ‘‘pump’’ mode. Putting in the slowly varying displacements and fields as before

$$x = X(t) e^{-i\omega_s t} + \text{c.c.} \quad (123)$$

$$E_i = \mathcal{E}_{0i}(t) e^{-i\omega_i t} + \text{c.c.} \quad (124)$$

$$E_p = \mathcal{E}_{0p} e^{-i\omega_p t} + \text{c.c.} \quad (125)$$

and taking the resonant terms, we find

$$\frac{d\mathcal{E}_{0i}}{dt} + \gamma_i \mathcal{E}_{0i} = \frac{i}{\tau} X^* \mathcal{E}_{0p} e^{-i\Delta\omega t} \quad (126)$$

where we make use of  $\Delta\omega \equiv \omega_p - \omega_i - \omega_s$ . Inserting the normalization used in [9] we find

$$\frac{dD_i}{dt} + \gamma_i D_i = \frac{i}{L} \frac{\omega_p^2}{\omega_i} X^* D_p e^{-i\Delta\omega t} \quad (127)$$

where we have used the fact that  $\tau = 2L/c$ , and  $k_p c = \omega_p$ . With the approximation that

$$\frac{\omega_p^2}{\omega_i} = \frac{\omega_p^2}{\omega_p - \omega_s} \approx \frac{\omega_p^2}{\omega_p} = \omega_p \quad (128)$$

(i.e.  $\omega_p \gg \omega_s$ ) we find,

$$\frac{dD_i}{dt} + \gamma_i D_i = \frac{iX^* D_p \omega_p}{L} e^{-i\Delta\omega t}. \quad (129)$$

This result is consistent with [9], eq. (1). For the detailed solutions to the coupled differential equations (118) and (129) and the condition for parametric amplification the reader is referred to [9]. The threshold condition is

$$\frac{2U_p Q_i Q_s}{mL^2 \omega_s^2} > 1 \quad (130)$$

where  $U_p$  is the energy stored in the ‘‘pump’’ mode,  $L$  is the length of the Fabry-Perot,  $m$  is the effective mass, and the  $Q$ ’s are the quality factors.

Note that the  $Q$ ’s are defined as follows

$$Q_s = \frac{\omega_s}{2\gamma_s}, \text{ ‘‘Mechanical’’ Oscillator} \quad (131)$$

$$Q_i = \frac{\omega_i}{2\gamma_i}, \text{ ‘‘Stokes’’ mode in FP} \quad (132)$$

$$Q_p = \frac{\omega_p}{2\gamma_p}, \text{ ‘‘Pump’’ mode in FP} \quad (133)$$

where the  $\gamma$ ’s correspond to the relaxation rate for each of the modes (i.e HWHM).

---

[1] M. Aspelmeyer, S. Gröblacher, K. Kammerer, and N. Kiesel, ‘‘Quantum Optomechanics—Throwing a Glance’’, *J. Opt. Soc. Am. B* **27**, A189 (2010).

[2] For previous experimental work on opto-mechanical parametric instabilities see [15, 16].

- [3] J. P. Gordon, H. J. Zeiger, and C. H. Townes, “Molecular Microwave Oscillator and New Hyperfine Structure in the Microwave Spectrum of  $\text{NH}_3$ ”, *Phys. Rev.* **95**, 282 (1954).
- [4] R.G. Maev, *Acoustic Microscopy* (John Wiley and Sons, New York, 2008), p.211.
- [5] Due to the finite time delay between successive bounces of the waves between the fixed mirror and the moving mirror, the action of the moving mirror upon the radiation contained in the cavity is non-adiabatic.
- [6] J. M. Manley and H. E. Rowe, “Some General Properties of Nonlinear Elements—Part I. General Energy Relations,” *Proc. IRE* **44**, 904–913 (1956).
- [7] H. van de Stadt and J.M. Muller “Multimirror Fabry-Perot interferometers” , *Opt. Soc. Am. A*, Vol. 2, No. 8, (1985)
- [8] S.J. Hogeveen, and Herman van de Stadt “Fabry-Perot Interferometers with Three Mirrors” , *Appl. Opt.* Vol. 25, No. 22, (1986)
- [9] V.B. Branginsky, S.E. Strigin, and S.P. Vyatchanin, “Parametric Oscillatory Instability in Fabry-Perot Interferometer” , *Phys. Lett. A* **287**, 331-338, (2001)
- [10] A reflection coefficient of 0.9999 can be achieved by using 9 double layer stack of ZnS ( $n = 2.35$ ) and  $\text{MgF}_2$  ( $n = 1.38$ ) coatings on mylar ( $n = 1.6$ ). For 700nm light this yields a thickness of 3.15 microns.
- [11] We select  $Q_s$  as a figure of merit based on published experimental work for superconducting cavities. However,  $Q_s$  depends sensitively on the fabrication procedure, and the design of the microwave cavity.
- [12] S. Kuhr, S. Gleyzes, C. Guerlin, J. Bernu, U.B. Hoff, S. Deléglise, S. Osnaghi, M. Brune, J.-M. Raimond, S. Haroche, E. Jacques, P. Bosland, and B. Visentin, “Ultrahigh Finesse Fabry-Perot Superconducting Resonator” , *Appl. Phys. Lett.* **90**, 164101 (2007)
- [13] H. Padamsee, J. Knobloch, and T. Hays, *RF Superconductivity for Accelerators* (2nd edition, Wiley-VCH Verlag GmbH & Co. KGaA, Weinheim 2008) p.159.
- [14] The mass is calculated from a 1.5 micron Nb coating, 3.15 micron multilayer dielectric reflection coating, and a 2 micron mylar drum thickness. As an order of magnitude we assume that in this high frequency regime the effective mass is on the order of the free mass (i.e. the pellicle acts as a free mass).
- [15] T. Corbitt, D. Ottaway, E. Innerhofer, J. Pelc, and N. Mavalvala “Measurement of Radiation-pressure-induced Optomechanical Dynamics in a Suspended Fabry-Perot Cavity” , *Phys. Rev. A* **74**, 021802(R) (2006)
- [16] T.J. Kippenberg, H. Rokhsari, T. Carmon, A. Scherer, and K.J. Vahala “Analysis of Radiation-Pressure Induced Mechanical Oscillation of an Optical Microcavity” *Phys. Rev. Lett.* **95**, 033901 (2005)
- [17] M.A. Bandres and J.C. Gutiérrez-Vega, “Ince-Gaussian Beams”, *Opt. Lett.* **29**, 144 (2004).
- [18] C.G. Chen, P.T. Konkola, J. Ferrera, R.K. Heilmann, and M. Schattenberg, “Analyses of Vector Gaussian Beam Propagation and the Validity of Paraxial and Spherical Approximations”, *J. Opt. Soc. Am. A* **19**, 404 (2002). Note that their initial *Ansatz*, i.e., their Eq. (6), with  $E_x \neq 0$  at  $z = 0$ , cannot

satisfy the conducting boundary conditions at  $z = 0$  in our Fig. 1, since, according to this *Ansatz*, the tangential component of the electric field  $E_x \neq 0$  would fail to vanish at the superconducting surface of the flat SC mirror located at  $z = 0$ . A nonvanishing tangential component  $E_x \neq 0$  just outside of the SC surface at  $z = 0$  would drive *infinite* supercurrents just beneath the SC surface at  $z = 0$ . Therefore, although their *Ansatz* with  $E_x \neq 0$  at  $z = 0$  might be appropriate for multilayer dielectric mirrors that are commonly used in laser resonators, it would not be appropriate for metallic mirrors, and certainly not for the SC mirrors of the microwave resonator in Fig. 1.

- [19] J.D. Jackson, *Classical Electrodynamics* (4th edition).
- [20] This is justified because the binding energy of the net charge of electrons to the surface of the metal is on the order of tens of eV, whereas the simple harmonic motion of the mirror corresponds to an energy on the order of meV.
- [21] M.J. Lawrence, B. Willke, M.E. Husman, E.K. Gustafson, and R.L. Byer “Dynamic response of a Fabry-Perot interferometer” J. Opt. Soc. Am. B, Vol 16, No. 4 (1999)
- [22] J. Cooper “Scattering of Electromagnetic Fields by a Moving Boundary: The One-Dimensional Case” IEEE Trans. Antennas Propagat., Vol. AP-28, No. 6, (1980)
- [23] M. Rakhmanov, R.L. Savage Jr., D.H. Reitze, D.B. Tanner “Dynamic resonance of light in Fabry-Perot cavities” Phys. Lett. A **305** (2005)239-244